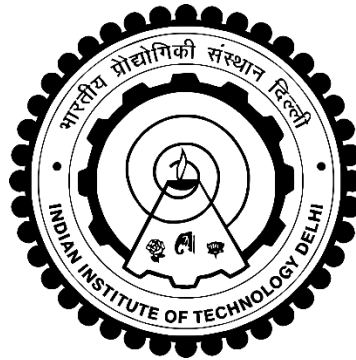


**EXPERIMENTAL AND NUMERICAL STUDIES ON
FLAT STRUCTURAL PANELS**

AMIT KUMAR



**DEPARTMENT OF APPLIED MECHANICS
INDIAN INSTITUTE OF TECHNOLOGY DELHI**

MAY 2020

©Indian Institute of Technology Delhi (IITD), New Delhi, 2020

EXPERIMENTAL AND NUMERICAL STUDIES ON FLAT STRUCTURAL PANELS

by

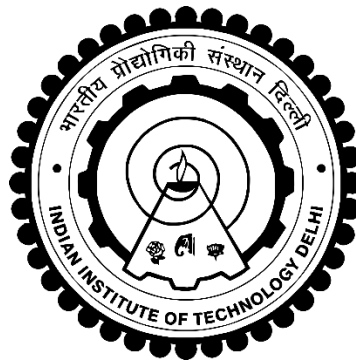
AMIT KUMAR

Department of Applied Mechanics

Submitted

in fulfilment of requirements for the degree of Doctor of Philosophy

to the



INDIAN INSTITUTE OF TECHNOLOGY DELHI

MAY 2020

Dedicated to

My grandfather Late Mr Babu Lal (Nanna) and Late Mr. Ambika Prasad (Dadda)

CERTIFICATE

This is to certify that the thesis entitled, “**EXPERIMENTAL AND NUMERICAL STUDIES ON FLAT STRUCTURAL PANELS**” submitted by **Mr. Amit Kumar** for the award of degree of **Doctor of Philosophy** to the **Indian Institute of Technology Delhi** is a record of bonafide research work carried out by him under our guidance and supervision.

Mr. Amit Kumar has fulfilled all the prescribed requirements and the thesis is, in our opinion, worthy of consideration for the degree of Doctor of Philosophy in accordance with the regulations of the Institute. The contents of this thesis have not been submitted in part or in full to any other University or Institute for the award of any degree or diploma.

Dr. M. K. Singha

Professor

Department of Applied Mechanics

Indian Institute of Technology Delhi

New Delhi-110016

India

Dr. Vikrant Tiwari

Assistant Professor

Department of Applied Mechanics

Indian Institute of Technology Delhi

New Delhi-110016

India

Place: New Delhi

Date:

ACKNOWLEDGMENTS

“Teachers use themselves as bridges over which they invite their students to cross; then, having facilitated their crossing, joyfully collapse, encouraging them to create bridges of their own”

I would like to express my sincere gratitude to my supervisors Prof. Maloy K Singha and Prof. Vikrant Tiwari for their expert guidance, inspiration, support and continuous encouragement. This work would not have been possible without their guidance and support. Their wisdom, knowledge, intellectual and moral support at every stage of my research enabled me to complete my research work.

Prof. Singha and Prof. Tiwari are a very kind-hearted person and very much friendly. I never hesitated to share any of my problems with them. I always got a solution from them. They are not only good researchers but also a person who never makes me hopeless. I was always confident that one day the research would be completed and this hope was because of them. Words cannot express how much they have influenced me. I thank them sincerely for caring so much.

Besides my supervisors, I would also like to thank my student research committee members Prof. Suhail Ahmad, Prof. B. P. Patel and Prof. Vasant Matsagar for their valuable suggestions throughout the research work.

There have been very few people who have touched my soul but among all Mr. Akhilesh Yadav (Former Chief Minister of Uttar Pradesh) deserves a special mention here. I have always looked up to him for inspiration. He always motivates me to not give up even in the worst situations. He is absolutely a dynamic personality. There cannot be anyone like him. My deepest regards for all that he has taught me. I owe him my life.

I would like to gratitude Dr. Prince Sharma and Mr. Shiv Poojan Yadav for their continuous encouragement, support and for giving their valuable time.

I would like to acknowledge the support of my friends Danish, Sanjay, Gargi, Purnashis, Anoop and Kuldeep in the most difficult phase of my Ph.D. and helped me to maintain a positive mindset. I have also made some wonderful friends during my research work at IIT Delhi. I wish to thank Aswani, Gaurav, Mohit, Adnan, Babu, Anuj, Anurag, Bashir, Sriram, Hassan, Wahi, Yadwinder, Mayank, Emarti, Ankita and Rishabh for their continuous support.

I would also like to acknowledge my childhood friends Dr. Dileep, Patel, Shailendra, Pradeep, Ravi Prakash, Kushagra, Mohit Makkar, Rahil and Dushyant. Who was always ready to help in any kind of problem.

Thanks are also due for Mr. Madan and Mr. Rishi for their help in conducting experiments at the “workshop” and “strength of materials” lab in the Department.

Sometimes things are not clear right away and people are very much nervous. At that time patience and hard work are the only way to achieve your goal. During my research work, I have faced such a situation. In that condition, I always remind my mind, the struggle and patience of my father Mr. Ashok Kumar and my uncle Mr. Veersen Yadav and this strengthen me to become more patient.

Finally, I would like to thank my parents and family members for their sacrifices in financing my education despite having great economic constraints. They encouraged me at every step by spending their significant time. Their unconditional love and blessings have enabled me to reach this point in my life.

Amit Kumar

ABSTRACT

The present thesis deals with the *large in-plane and out-of-plane deformation behaviors* of flat structural panels under various loading conditions. The structural performance of such panels depends on the mechanical behavior of its constituent material, its geometry and loading conditions. An appropriate experimental procedure (experimental setup, specimen geometry and measurement technique) is required for the mechanical characterization of the material, while a suitable numerical model is necessary to simulate the in-plane and transverse deformations of the commonly used flat panels in civil, mechanical and aircraft structures. The present thesis is an attempt to examine the suitability of different specimen geometries for the "*material characterization*" and employ an appropriate numerical technique for the "*nonlinear analysis of non-rectangular plates*".

In the beginning, an extensive experimental investigation is conducted on aluminum (A11100) and mild steel (IS 1570) plates under various in-plane loading (tension, shear and combined tension and shear) conditions using the modified Arcan fixture. The full-field displacement and strain profiles of metallic specimens under in-plane loading are obtained using the three-dimensional digital image correlation (DIC). Four different geometries of the specimens are judiciously selected, so that some of the specimens undergo large in-plane strain without significant out-of-plane deformation, while the other specimens buckle during the in-plane plastic deformation. In the absence of plastic buckling, the constitutive relations of aluminum (A11100) and mild steel (IS 1570) plates under pure tension and pure shear are obtained. The corresponding material properties are subsequently used to simulate the elastic / plastic buckling loads of other sets of specimen shapes and the flexural behavior of different flat panels. The presence of in-plane shear stress significantly reduces the ultimate tensile strength of both

aluminum and mild steel plates. The mild steel specimens show a higher tendency for out-of-plane buckling compared to aluminum specimens, as the hardening exponent is higher for mild steel.

Next, an effort is made to develop a numerical model for the linear and nonlinear analyses of shear deformable quadrilateral plates. The Reissner-Mindlin quadrilateral plates are discretized with quadrilateral background cells. Then, the membrane and bending stiffness matrices are evaluated using the *edge-based smoothed finite element method* (ES-FEM). The shear stiffness matrix is separately obtained for four-node quadrilateral plate bending elements using a proposed "*cell-based smoothed transverse shear strain approach*". An in-house MATLAB code is developed, and the convergence, accuracy and distortion-sensitivity of the proposed smoothing algorithm are found to be good for the linear analysis of thin and moderately thick arbitrary quadrilateral plates. The performance of the proposed "*smoothed shear strain approach*" is compared with the existing "*edge-consistent shear strain technique*" and "*MITC (mixed interpolation of tensorial components) approach*" for the four-node quadrilateral plate bending element.

Thereafter, the bending, buckling and vibration behaviors of isotropic (mild steel) rectangular, trapezoidal and quadrilateral plates are taken up for investigation. Both the edge compression and edge shear are considered for the stability analysis of rectangular and trapezoidal panels after estimating the exact pre-buckling in-plane stress resultants. The linear elastic flexural analysis for isotropic flat panels is extended to geometrically non-linear bending, post-buckling and large amplitude free vibration behaviors of non-rectangular flat panels. The bending stiffness of trapezoidal and quadrilateral plates significantly increases with the reduction of one of its edge-length, while the lengths of the other three edges are kept nearly constant. An attempt is also made to study the plastic buckling behavior of thick aluminum (A1100) and mild steel (IS 1570) panels under in-

plane shear. The numerical study is also extended to quadrilateral plates made of laminated composite materials with idealistic materials properties. An attempt is also made to present the numerical results in non-dimensional form for easy reference to engineers and researchers working on the non-rectangular panels.

सार

वर्तमान थीसिस विभिन्न लोडिंग परिस्थितियों में फ्लैट संरचनात्मक पैनलों के बड़े इन-प्लेन और आउट-ऑफ-प्लेन विरूपण व्यवहारों से संबंधित है। ऐसे पैनलों का संरचनात्मक प्रदर्शन इसकी घटक सामग्री, इसकी ज्यामिति और लोडिंग की स्थिति के यांत्रिक व्यवहार पर निर्भर करता है। सामग्री के यांत्रिक लक्षण वर्णन के लिए एक उपयुक्त प्रयोगात्मक प्रक्रिया (प्रयोगात्मक सेटअप, नमूना ज्यामिति और माप तकनीक) की आवश्यकता होती है, जबकि सिविल, मैकेनिकल और विमान संरचनाओं में आमतौर पर उपयोग किए जाने वाले फ्लैट पैनलों के इन-प्लेन और अनुप्रस्थ विकृति का अनुकरण करने के लिए एक उपयुक्त संख्यात्मक मॉडल आवश्यक है। वर्तमान थीसिस "सामग्री लक्षण वर्णन" के लिए अलग-अलग नमूना ज्यामिति की उपयुक्तता की जांच करने और "गैर-आयताकार प्लेटों के गैर-रेखीय विश्लेषण" के लिए एक उपयुक्त संख्यात्मक तकनीक का उपयोग करने का प्रयास है।

शुरुआत में, संशोधित आर्कन स्थिरता का उपयोग करके विभिन्न इन-प्लेन लोडिंग (तनाव, कतरनी और संयुक्त तनाव और कतरनी) स्थितियों के तहत एल्यूमीनियम (AI 1100) और हल्के स्टील (IS 1570) प्लेटों पर एक व्यापक प्रयोगात्मक जांच की जाती है। पूर्ण-क्षेत्र विस्थापन और मेटालिक नमूनों के तनाव प्रोफाइल को इन-प्लेन लोडिंग के तहत त्रि-आयामी डिजिटल छवि सहसंबंध (डीआईसी) का उपयोग करके प्राप्त किया जाता है। नमूनों के चार अलग-अलग ज्यामिति को विवेकपूर्ण रूप से चुना गया है (डिजाइन किया गया है), ताकि कुछ नमूने महत्वपूर्ण आउट-ऑफ-प्लेन विरूपण के बिना बड़े इन-प्लेन तनाव से गुजरें, जबकि अन्य नमूने इन-प्लेन प्लास्टिक विरूपण के दौरान बकसुआ बनाते हैं। प्लास्टिक बकलिंग की अनुपस्थिति में, शुद्ध तनाव और शुद्ध कतरनी के तहत एल्यूमीनियम (AI 1100) और हल्के स्टील (IS 1570) प्लेटों के संवैधानिक संबंध प्राप्त होते हैं। तत्संबंधी भौतिक गुणों का उपयोग बाद में नमूनों के आकार के अन्य सेटों के लोचदार / प्लास्टिक बकलिंग भार और विभिन्न फ्लैट पैनलों के लचीले व्यवहार का अनुकरण करने के लिए किया जाता है। इन-प्लेन शीयर स्ट्रेस की उपस्थिति एल्यूमीनियम और हल्के स्टील प्लेटों की अंतिम तन्य शक्ति को काफी कम कर देती है। हल्के स्टील के नमूनों में एल्यूमीनियम नमूनों की तुलना में आउट-ऑफ-प्लेन बकलिंग के लिए उच्च प्रवृत्ति दिखाई देती है, क्योंकि हल्के स्टील के लिए सख्त घातांक अधिक होता है।

इसके बाद, कतरनी विकृति चतुर्भुज प्लेटों के रेखिक और अरेखीय विश्लेषण के लिए एक संख्यात्मक मॉडल विकसित करने का प्रयास किया जाता है। रीनसर माइंडलिन चतुर्भुज प्लेटों को चतुर्भुज पृष्ठभूमि कोशिकाओं के साथ पृथक किया जाता है। फिर, झिल्ली और झुकने कठोरता आव्यूह का मूल्यांकन धार आधारित चिकने परिमित तत्व

विधि (ES-FEM) का उपयोग करके किया जाता है। कतरनी कठोरता मैट्रिक्स चार-नोड चतुर्भुज प्लेट झुकने वाले तत्वों के लिए एक प्रस्तावित "सेल-आधारित चिकनी अनुप्रस्थ कतरनी तनाव दृष्टिकोण" का उपयोग करके अलग से प्राप्त किया जाता है। इन-हाउस MATLAB कोड विकसित किया गया है, और प्रस्तावित चौरसाई एल्गोरिथ्म के अभिसरण, सटीकता और विरूपण-संवेदनशीलता की जांच पतली और मध्यम मोटी मनमानी चतुर्भुज प्लेटों के रैखिक विश्लेषण के लिए की जाती है। प्रस्तावित "स्मूद शीयर स्ट्रेन एप्रोच" की तुलना चार-नोड चतुर्भुज प्लेट झुकने वाले तत्व के लिए मौजूदा "एज-सुसंगत शीयर स्ट्रेन तकनीक" और "एमआईटीसी (टेंसरियल घटकों के मिश्रित प्रक्षेप) दृष्टिकोण" से की जाती है।

तत्पश्चात, आइसोट्रोपिक (माइल्ड स्टील) आयताकार, ट्रेपेज़ॉइडल और चतुर्भुज प्लेटों के झुकने, बकलिंग और कंपन व्यवहार को जांच के लिए लिया जाता है। सटीक पूर्व बकसुआ इन-प्लेन तनाव परिणामी का अनुमान लगाने के बाद आयताकार और ट्रेपेज़ॉइडल पैनलों के स्थिरता विश्लेषण के लिए एज कंप्रेशन और एज शीयर दोनों का ध्यान रखा गया। आइसोट्रोपिक प्लैट पैनलों के लिए रैखिक लोचदार फ्लेक्सुरल विश्लेषण को ज्यामितीय रूप से गैर-रैखिक झुकने, पोस्ट-बकलिंग और गैर-आयताकार प्लैट पैनलों के बड़े आयाम मुक्त कंपन व्यवहारों तक बढ़ाया जाता है। ट्रेपेज़ॉइडल और चतुर्भुज प्लेटों की झुकने की कठोरता इसकी बढ़त-लंबाई में से एक की कमी के साथ काफी बढ़ जाती है, जबकि अन्य तीन किनारों की लंबाई लगभग स्थिर रहती है। इन-प्लेन शीयर के नीचे मोटे एल्यूमीनियम (Al 1100) और हल्के स्टील (IS 1570) पैनलों के प्लास्टिक बकलिंग व्यवहार का अध्ययन करने का भी प्रयास किया गया है। संख्यात्मक अध्ययन को आदर्शवादी सामग्री गुणों के साथ टुकड़े टुकड़े में मिश्रित सामग्री से बने चतुर्भुज प्लेटों तक भी विस्तारित किया गया है। गैर-आयताकार पैनल पर काम करने वाले इंजीनियरों और शोधकर्ताओं के आसान संदर्भ के लिए संख्यात्मक परिणामों को गैर-आयामी रूप में प्रस्तुत करने का प्रयास भी किया गया है।

CONTENTS

Certificate	i
Acknowledgments	iii
Abstract	v
Contents	xi
List of Figures	xv
List of Tables	xxi
List of Symbols	xxv
CHAPTER 1	
INTRODUCTION	1
CHAPTER 2	
LITERATURE REVIEW	5
2.1 Introduction	5
2.2 Experimental Technique for The In-Plane Loading	5
2.3 Structural Behaviour of Quadrilateral Panels	10
Bending of Quadrilateral Panels	10
Stability Analysis of Quadrilateral Panels	11
Free Vibration Analysis of Quadrilateral Panels	14
Numerical Methods for the Analysis of Quadrilateral Panels	15
2.4 Summary	19

CHAPTER 3

SCOPE AND OBJECTIVE	21
A Experimental Characterization of the Flat Panels Under In-Plane Loading	21
B Bending, Buckling and Vibration Analyses of Quadrilateral Panels	22

CHAPTER 4

EXPERIMENTAL TECHNIQUE AND FEM MODEL	25
4.1 Introduction	25
4.2 Experimental Procedure	25
4.2.1 The Proposed Geometries of the Arcan Specimen	26
4.2.2 Material Details	27
4.2.3 Fixture Details	29
4.2.4 Measurement Technique (3D DIC)	30
4.2.5 Loading Details	32
4.2.6 Stress Triaxiality <i>versus</i> Fracture Strain	32
4.3 Finite Element Model	35
4.3.1 Constitutive Modelling	37
4.3.2 Failure Model	38

CHAPTER 5

FINITE ELEMENT FORMULATION	41
5.1 Introduction	41
5.2 Finite Element Formulation	41

5.2.1	Edge Based Smooth Finite Element Method	43
5.2.2	Edge-consistent Shear Strain Interpolation for Quadrilateral Elements	47
5.2.3	Smoothed Shear Strain Approach	47
5.2.4	The nonlinear Equations of Equilibrium	48
5.3	Solution Procedure	49
5.3.1	Nonlinear Bending Analysis	49
5.3.2	Stability Analysis	51
5.3.3	Nonlinear Free vibration	53
CHAPTER 6		
MATERIAL RESPONSE CHARACTERIZATION		55
6.1	Introduction	55
6.2	The Motivation	55
6.3	Problem Statement	56
6.4	Experimental Observations	57
6.4.1	Pure Shear Loading	58
6.4.2	Mix mode (30° and 60°) and Tensile (90°) Loading	74
6.5	Numerical Simulation	81
6.6	Summary	87
CHAPTER 7		
STRUCTURAL BEHAVIOUR OF NON-RECTANGULAR PANELS		89

7.1	Introduction	89
7.2	Validation and Convergence Study	89
7.3	Bending Analysis of The Quadrilateral Panels	100
7.4	Buckling Analysis of the Quadrilateral Panels	106
7.5	Vibration Analysis of Quadrilateral Panels	122
7.6	Summary	131
CHAPTER 8		
CONCLUSION		133
8.1	Experimental Investigation	133
8.2	Numerical Modeling of Quadrilateral Plates	135
8.3	Structural Behavior of Quadrilateral Plates	135
8.4	Recommendation for Future Work	136
REFERENCES		139
APPENDIX 1		155
LIST OF PUBLICATIONS BY MR. AMIT KUMAR (AUTHOR)		157
AUTHOR BIODATA		159

LIST OF FIGURES

Fig 4.2.1.	Arcan specimen geometries used in pure shear and mixed mode (I/II) loading (a) Smooth arc butterfly specimen with 39 mm wide central cross-section (b) Smooth arc butterfly specimen with 19 mm wide central cross-section (c) V-shaped specimen with 19 mm wide central cross-section (d) Smooth arc butterfly specimen with a central notch leaving a 19 mm central cross-section.	26
Fig 4.2.2.	Sequential assembly of Arcan fixture with the specimen.	28
Fig 4.2.3.	Schematic representation of 3D stereo-vision coordinate system used in the analysis of the images.	31
Fig 4.2.4.	Experimental set-up used in the full field 3-D DIC measurement and the images of the specimen being loaded at different angles.	33
Fig 4.2.5.	(a) Geometry and actual image of the tensile test specimens used in stress triaxiality measurement. Stress triaxiality <i>versus</i> fracture strain response of (b) Aluminium and (c) Mild Steel	35
Fig 4.3.1.	Mesh pattern and density distribution for all the considered specimens	36
Fig 4.3.2.	Convergence study of mild steel and aluminium specimens (l_e is the element length)	37
Fig 5.2.1.	Schematic representation of the edge-based smoothing domain of quadrilateral elements (field nodes are encircled).	43
Fig 5.2.2.	Schematic representation of the tangential shear strains in a quadrilateral element.	45
Fig 5.2.3	Schematic representation of the discrete shear gap in a quadrilateral element	47
Fig 5.3.1.	Geometry of square panel subject to in-plane edge loads.	51
Fig 6.3.1.	Results obtained through 3D DIC for the full-field shear strain (ϵ_{xy}) distribution on a (a) Aluminium AL1100 specimen, (b) Mild steel IS1570 specimen, and their corresponding full-field out-of-plane displacement (w) for (c) aluminium 1100, (d) mild steel IS1570, under the identical experimental conditions.	57

Fig 6.4.1.	The shear stress <i>versus</i> shear strain response of Aluminium and mild steel specimens under pure shear loading by the Arcan fixture ($\theta = 0^\circ$).	58
Fig 6.4.2.	Full field out-of-plane displacement profile (w : obtained from 3D DIC) of aluminium butterfly specimen (shape-1) under pure shear loading by the Arcan fixture ($\theta = 0^\circ$).	62
Fig 6.4.3.	Full field shear strain distribution (ε_{xy} : obtained from 3D DIC) of aluminium butterfly specimen (shape-1) under pure shear loading by the Arcan fixture ($\theta = 0^\circ$).	63
Fig 6.4.4.	Full field out-of-plane displacement profile (w : obtained from 3D DIC) of mild steel butterfly specimen (shape-1) under pure shear loading by the Arcan fixture ($\theta = 0^\circ$).	64
Fig 6.4.5.	Full field shear strain distribution (ε_{xy} : obtained from 3D DIC) of mild steel butterfly specimen (shape-1) under pure shear loading by the Arcan fixture ($\theta = 0^\circ$).	65
Fig 6.4.6.	Full field out-of-plane displacement profile (w : obtained from 3D DIC) of mild steel double-notch specimen (shape-4) under pure shear loading by the Arcan fixture ($\theta = 0^\circ$).	67
Fig 6.4.7.	Full field shear strain distribution (ε_{xy} : obtained from 3D DIC) of mild steel double-notch specimen (shape-4) under pure shear loading by the Arcan fixture ($\theta = 0^\circ$).	68
Fig 6.4.8a.	Full field strain distribution (ε_{xx} : obtained from 3D DIC) of different specimen shapes under pure shear loading by the Arcan fixture ($\theta = 0^\circ$).	71
Fig 6.4.8b.	Full field strain distribution (ε_{yy} : obtained from 3D DIC) of different specimen shapes under pure shear loading by the Arcan fixture ($\theta = 0^\circ$).	72
Fig 6.4.8c.	Full field shear strain distribution (ε_{xy} : obtained from 3D DIC) of different specimen shapes under pure shear loading by the Arcan fixture ($\theta = 0^\circ$).	73

Fig 6.4.9.	The shear stress <i>versus</i> shear strain response of Aluminium and mild steel specimens under Mixed mode loading by the Arcan fixture ($\theta = 30^\circ$).	75
Fig 6.4.10.	The tensile stress <i>versus</i> strain response of Aluminium and mild steel specimens under Mixed mode loading by the Arcan fixture ($\theta = 60^\circ$).	75
Fig 6.4.11.	The stress <i>versus</i> Strain response at different pull rates for aluminium specimens.	77
Fig 6.4.12.	The stress <i>versus</i> Strain response at different pull rates for mild steel specimens.	78
Fig 6.4.13.	The shear stress <i>versus</i> shear strain and tensile stress <i>versus</i> tensile strain responses of double-V shape (specimen 3) aluminum (AL) and mild steel (MS) specimens at different load angles.	79
Fig 6.5.1.	Full field shear strain distribution (ε_{xy} : obtained from FE simulation) of aluminium butterfly specimen (shape-1) under pure shear loading by the Arcan fixture ($\theta = 0^\circ$).	82
Fig 6.5.2.	Full field shear strain distribution (ε_{xy} : obtained from FE simulation) of mild steel butterfly specimen (shape-1) under pure shear loading by the Arcan fixture ($\theta = 0^\circ$).	83
Fig 6.5.3.	Full field shear strain distribution (ε_{xy} : obtained from FE simulation) of mild steel double-notch specimen (shape-4) under pure shear loading by the Arcan fixture ($\theta = 0^\circ$).	84
Fig 6.5.4.	Comparison between experimental and FE simulation stress-strain response for mild steel specimens.	85
Fig 6.5.5.	Comparison between experimental and FE simulation stress-strain response for aluminium specimens.	86
Fig 7.2.1.	Geometry, loading and boundary conditions of different quadrilateral plates	91
Fig 7.2.2.	Finite Element mesh for the trapezoidal plate.	92

Fig 7.2.3.	Postbuckling response of square plates. (a) Isotropic square ($a/h = 1000$) plate under in-plane compression (b) Angle-ply $[45^\circ/-45^\circ/-45^\circ/45^\circ]$ composite square ($a/h = 100$) plate under in-plane shear ($E_I/E_T = 10$, $G_{IT}/E_T = 0.25$, $\mu = 0.3$).	99
Fig 7.3.1.	Non-dimensional central deflection (w_{\max}/h) of cross ply $[0^\circ/90^\circ/90^\circ/0^\circ]$ laminated composite trapezoidal plate ($a/h = 100$, $b/a = 1$) subjected to a uniformly distributed load q_0 . ($Q=q_0a^4/E_2h^4$).	101
Fig 7.3.2.	Non-dimensional central deflection (w_{\max}/h) of a cross ply $[45^\circ/-45^\circ/-45^\circ/45^\circ]$ laminated composite trapezoidal plate ($a/h = 100$, $b/a = 1$) subjected to a uniformly distributed load q_0 . ($Q=q_0a^4/E_2h^4$).	102
Fig. 7.3.3.	Dimensionless maximum deflection (w_{\max}/h) of a cross ply $[0^\circ/90^\circ/90^\circ/0^\circ]$ laminated composite quadrilateral plate ($a/h = 100$) subjected to a uniformly distributed load q_0 . ($Q=q_0a^4/E_2h^4$)	104
Fig 7.3.4.	Dimensionless maximum deflection (w_{\max}/h) of a cross ply $[45^\circ/-45^\circ/-45^\circ/45^\circ]$ laminated composite quadrilateral plate ($a/h = 100$) subjected to a uniformly distributed load q_0 . ($Q=q_0a^4/E_2h^4$).	105
Fig 7.4.1.	The postbuckling response of simply supported trapezoidal plates under in-plane compressive load. ($a/h = 100$).	113
Fig 7.4.2.	The postbuckling response of simply supported trapezoidal plates under in-plane shear load ($a/h = 100$).	114
Fig 7.4.3.	The postbuckling response of isotropic arbitrary quadrilateral plates under in-plane compression and in-plane shear.	116
Fig 7.4.4.	The postbuckling response of simply supported arbitrary quadrilateral plate under in-plane compressive load ($a/h = 100$).	117
Fig 7.4.5.	The postbuckling response of simply supported arbitrary quadrilateral plate under in-plane shear load ($a/h = 100$).	118
Fig 7.4.6.	Post Buckling response of mild steel square plate under in-plane edge shear loading.	120

Fig 7.4.7. Post Buckling response of Aluminium square plate under in-plane edge shear load.

121

LIST OF TABLES

Table 4.2.1.	The chemical composition of Aluminium 1100 and Mild steel IS 1570 specimens.	27
Table 4.2.2.	Important parameters related to the Imaging Setup.	31
Table 6.4.1.	The in-plane strain and out-of-plane deformation of aluminium (AL-1100) specimens at various stages of shear loading.	59
Table 6.4.2.	The in-plane strain and out-of-plane deformation of Mild Steel (IS 1570) specimens at various stages of shear loading.	60
Table 6.4.3.	Shape dependent specimen strain and displacement (w) data for IS-1570 and AL-1100 for 1mm/min loading rate.	76
Table 7.2.1.	Convergence of non-dimensional maximum displacement ($\bar{w}=10000w_c D / q_0 a^4$) for thin ($a/h = 1000$) isotropic un-symmetric trapezoidal plate (Fig 7.2.1a) under uniformly distributed transverse load q_0 .	94
Table 7.2.2.	Convergence of centroidal displacement of an isotropic irregular quadrilateral plate under uniformly distributed transverse load q_0 . ($D = 1, q_0 = 1, a/h = 500$).	94
Table 7.2.3.	Convergence of non-dimensional buckling load ($\lambda_{cr}/\lambda_{cr0}$; λ_{cr0} is the critical buckling load of a square plate) for a clamped (CCCC) symmetric trapezoidal plate subjected to in-plane compressive edge load. ($b/h = 100, c/b = 1$).	95
Table 7.2.4.	Non-dimensional critical buckling load ($\lambda_{cr} = Pa / \pi^2 D$) of isotropic trapezoidal plates. ($a/b = 1$; $P = c.N_{yy}$ or $P = c.N_{xy}$ for symmetric trapezoid $P = a.N_{yy}$ or $P = a.N_{xy}$ un-symmetric trapezoid).	96
Table 7.2.5.	Comparison of non-dimensional vibration frequency ($\varpi = \omega b^2 \sqrt{\rho h / D} / \pi^2$) for thin ($a/h = 1000$; $b = a$) isotropic quadrilateral plate (Fig 7.2.1).	97
Table 7.2.6.	Comparison of non-dimensional central displacement ($\bar{w} = w_{max} / h$) with non-dimensional load parameter ($\bar{q} = q_0 L_y / Eh^4$) of a clamped symmetric trapezoidal plate	98

	subjected to a uniformly distributed load q_0 . ($a/c = 3$, $b/a = 0.577$, $a/h = 1000$, $L_y = a/1.5$).	
Table 7.2.7.	Comparison of nonlinear frequency ratio (ω_{NL}/ω_L) of thin square plate ($a=b$; $a/h=100$) with simply supported boundary condition.	98
Table 7.4.1.	Non-dimensional critical buckling load ($\lambda_{cr} = Pa / \pi^2 D$) of isotropic trapezoidal plates. ($a/b = 1$; $P = c.N_{yy}$ or $P = c.N_{xy}$ for symmetric trapezoid $P = a.N_{yy}$ or $P = a.N_{xy}$ un-symmetric trapezoid).	107
Table 7.4.2.	Non-dimensional critical buckling load ($\lambda_{cr} = Pa / E_T h^3$) of laminated composite $[0^\circ/90^\circ/90^\circ/0^\circ]$ trapezoidal plates. ($a/b=1$; $P = c.N_{yy}$ or $P = c.N_{xy}$ for symmetric trapezoid $P = a.N_{yy}$ or $P = a.N_{xy}$ un-symmetric trapezoid).	108
Table 7.4.3.	Non-dimensional critical buckling load ($\lambda_{cr} = Pa / E_T h^3$) of laminated composite $[45^\circ/-45^\circ/-45^\circ/45^\circ]$ trapezoidal plates. ($a/b = 1$; $P = c.N_{yy}$ for symmetric trapezoid and $P = a.N_{yy}$ for un-symmetric trapezoid).	109
Table 7.4.4.	Non-dimensional buckling load parameter ($\lambda_{cr} = Pa / \pi^2 D$) for isotropic quadrilateral plate under in-plane edge load.	110
Table 7.4.5.	Non-dimensional buckling load parameter ($\lambda_{cr} = Pa / E_T h^3$ for laminated composite) quadrilateral laminated composite $[0^\circ/90^\circ/90^\circ/0^\circ]$ plate under in-plane edge load.	111
Table 7.4.6.	Non-dimensional buckling load parameter ($\lambda_{cr} = Pa / E_T h^3$ for laminated composite) quadrilateral laminated composite $[45^\circ/-45^\circ/-45^\circ/45^\circ]$ plate under in-plane edge load.	112
Table 7.5.1.	Non-dimensional frequencies ($\varpi = \omega a^2 / h \sqrt{\rho / E_2}$) of four-layer $[0^\circ/90^\circ/90^\circ/0^\circ]$ laminated composite thin ($a/h = 100$) trapezoidal plates.	123
Table 7.5.2.	Non-dimensional frequencies ($\varpi = \omega a^2 / h \sqrt{\rho / E_2}$) of four-layer $[45^\circ/-45^\circ/-45^\circ/45^\circ]$ laminated composite thin ($a/h = 100$) trapezoidal plates.	124

Table 7.5.3.	Non-dimensional frequencies ($\bar{\omega} = \omega a^2 / h \sqrt{\rho / E_2}$) for four-layer $[0^0/90^0/90^0/0^0]$ laminated composite thin ($a/h = 100$) Quadrilateral plates (Fig 7.2.1c).	125
Table 7.5.4.	Non-dimensional frequencies ($\bar{\omega} = \omega a^2 / h \sqrt{\rho / E_2}$) for four-layer $[45^\circ/-45^\circ/-45^\circ/45^\circ]$ laminated composite thin ($a/h = 100$) Quadrilateral plates (Fig 7.2.1c).	126
Table 7.5.5.	The nonlinear frequency ratios (ω_{NL}/ω_L) of 4-layer $[0^0/90^0/90^0/0^0]$ thin ($a/h = 100$) laminated quadrilateral plates with different boundary condition.	127
Table 7.5.6.	The nonlinear frequency ratios (ω_{NL}/ω_L) of 4-layer $[45^\circ/-45^\circ/-45^\circ/45^\circ]$ thin ($a/h = 100$) laminated quadrilateral plates with different boundary condition.	128
Table 7.5.7.	The nonlinear frequency ratios (ω_{NL}/ω_L) of 4-layer $[0^0/90^0/90^0/0^0]$ thin ($a/h = 100$) laminated quadrilateral plates with different boundary condition.	129
Table 7.5.8.	The nonlinear frequency ratios (ω_{NL}/ω_L) of 4-layer $[45^\circ/-45^\circ/-45^\circ/45^\circ]$ thin ($a/h = 100$) laminated quadrilateral plates with different boundary condition.	130

LIST OF SYMBOLS

E	Young's modulus
μ	Poisson's Ratio
G	Shear modulus
ρ	Density of the material
σ	Stress field in the structure
σ_y	Yield strength of the material
σ_{uT}	Ultimate tensile strength of the material
σ_{us}	Ultimate shear strength of the material
G_s	secant shear modulus
ε	Strain field in the structure
ε_{xy}	Shear strain
ε_b	Bending strain
ε_s	Shear strain
ε_m^L	Linear component of membrane strain
ε_m^{NL}	Nonlinear component of membrane strain
ε_{eq}	Equivalent plastic strain
σ^*	Stress tri-axiality ratio
G_f	Dissipated fracture energy
θ_x	Rotation of mid plane about the Y-axis
θ_y	Rotation of mid plane about the X-axis
U_m	Membrane strain energy
U_b	Bending strain energy
U_s	Shear strain energy
n_x, n_y	Direction cosine
γ_{sz}	Tangential shear strain
δ	Vector of degree of freedom
ω	Natural frequency of the structure
h	Thickness of the flat panel
a	Length of the structure
b	Width of the structure

f	Focal length of the lense
λ_{cr}	Non-dimensional critical buckling load